JOURNAL OF Materials CHEMISTRY

Synthesis of ultra-high purity trialkylgallium MOVPE precursors. Crystal structures of triethylgallium and triisopropylgallium adducts with macrocyclic tertiary amines

Kathleen M. Coward,[a] Anthony C. Jones,*[a] Alexander Steiner,[a] Jamie F. Bickley,[a] Martyn E. Pemble,[b] Neil M. Boag,[b] Simon A. Rushworth[c] and Lesley M. Smith[c]

[a]*Department of Chemistry, University of Liverpool, Liverpool, UK L69 7ZD. E-mail: tony@tjconsultancy.demon.co.uk; Fax: 0151 708 0662; Tel: 0151 794 3875; Tel: 0151 493 2441*
[b]*Department of Chemistry, University of Salford, Salford, UK M5 4WT*
[c]*Epichem Limited, Power Road, Bromborough, Wirral, UK CH62 3QF*

Received 10th March 2000, Accepted 16th May 2000
Published on the Web 29th June 2000

A synthesis and purification route has been developed for base-free trialkylgallium compounds which avoids the use of traditional ether solvents. The R_3Ga compound (R = Et, Pr^i) is synthesised in triethylamine, NEt_3, which leads to the adducts $R_3Ga(NEt_3)$. The NEt_3 ligand can be readily displaced by the addition of low volatility bidentate, tetradentate or hexadentate tertiary amines to give adducts of the type $(R_3Ga)_xL$ ($x = 2$, 4, 6), from which base-free R_3Ga compounds are obtained by mild thermal dissociation. The synthesis and characterisation of these adducts are described and crystal structures reported for the adducts between R_3Ga (R = Et, Pr^i) and the multidentate macrocyclic amines 1,4,8,11-tetramethyl-1,4,8,11-tetraazacyclotetradecane and 1,4,7,10,13,16-hexamethyl-1,4,7,10,13,16-hexaazacyclooctadecane. These are the first reported structural studies of the Et_3Ga and Pr^i_3Ga molecules in the solid state.

1 Introduction

Metalorganic chemical vapour phase epitaxy (MOVPE) has become the established technique for the deposition of III–V compound semiconductor layers used in a large variety of electronic devices, such as solid state lasers, light emitting diodes, infrared detectors and high mobility transistors.[1,2] For efficient and long-lasting semiconductor devices, it is essential that the III–V layers are extremely pure, with trace metal impurities (*e.g.* Si, Zn, Sn) and oxygen contamination reduced to levels below 1 ppm in the deposited layer. The purity of the III–V layers deposited by MOVPE is critically dependent on the purity of the group III metalorganic precursor,[3] and chemists have therefore had to develop new synthesis and purification techniques capable of producing ultra-high purity organometallic compounds.

The removal of trace metal impurities from an organometallic compound is difficult to achieve using "conventional" purification techniques, such as fractional distillation or zone refining. However, this problem has been largely overcome by the use of "adduct purification",[4–6] which involves the formation of an adduct between the group III trialkyl and an appropriate Lewis base[3] (typically a high boiling ether or a tertiary amine or phosphine). After removal of non-adducting or weakly-adducting impurities *in vacuo*, the purified organometallic is obtained by mild thermal dissociation of the adduct.[3]

Although adduct purification techniques are highly effective in removing trace metallic impurities from the organometallic precursor, they are less effective in removing trace oxygen contaminants. This is a serious problem, as the presence of a few ppm of oxygen in the III–V layers is particularly damaging in optoelectronic devices, such as light emitting diodes and lasers, resulting in a serious reduction in luminescence efficiency.[7] It has been shown that traces of diethyl ether, Et_2O, in the group III trialkyl precursor is a major source of oxygen contamination in AlGaAs and AlInAs layers grown by MOVPE or chemical beam epitaxy (CBE).[8,9] The trace Et_2O originates from the organometallic synthesis reaction, which usually involves the alkylation of a metal trihalide (MX_3) by a Grignard reagent (RMgX), or an alkyllithium compound (RLi).[10] The Et_2O subsequently forms an adduct with the R_3Ga or R_3In precursor and is difficult to displace completely using conventional adduct purification techniques. Therefore, for the manufacture of low oxygen content metal alkyls it is necessary to entirely eliminate Et_2O from the synthesis route.

Although R_3Ga and R_3In compounds can be synthesised *via* the reaction of MCl_3 and R_3Al in the absence of a solvent,[10] these routes involve the handling of large volumes of hazardous pyrophoric R_3Al starting material and it is also difficult to separate volatile residual R_2AlCl impurities from the R_3Ga or R_3In product. In addition, commercially available R_3Al reagents are generally of uncertain purity, often containing high levels of metallic and organic impurities, so that synthesis routes involving RMgX or RLi alkylating agents are preferred for the large scale manufacture of high purity R_3Ga and R_3In precursors.

It has been shown that Grignard reagents can be synthesised in trialkylamine solvents,[11] and we have thus developed a proprietary synthetic route to R_3M compounds (R = Ga, In) in which the ether solvent is replaced by trialkylamines such as NEt_3 and NMe_2Et.[8,12] This leads to adducts such as $Pr^i_3Ga(NEt_3)$, from which AlGaAs with significantly reduced oxygen contamination has been grown by CBE.[8,12] However, these adducts have low vapour pressures (< 1 Torr at 35 °C) which limits their widespread application in CBE or MOVPE. In a preliminary communication,[13] we described how NEt_3 can be readily displaced from $Pr^i_3Ga(NEt_3)$ and $Et_3Ga(NEt_3)$ by the addition of 4,4′-methylenebis(*N*,*N*′-dimethylaniline) (MBDA) or the multidentate aza-crown ligands 1,4,8,11-tetramethyl-1,4,8,11-tetraazacyclotetradecane (N_4-aza crown) and 1,4,7,10,13,16-hexamethyl-1,4,7,10,13,16-hexaazacyclooctadecane (N_6-aza crown). This leads to the adducts $(R_3Ga)_2$[MBDA], $(R_3Ga)_4$[N_4-aza crown] (R = Et,

DOI: 10.1039/b001937m

Pr^i), $(Et_3Ga)_4$[N_6-aza crown], $(Et_3Ga)_6$[N_6-aza crown] and $(Pr^i_3Ga)_4$[N_6-aza crown], from which the base-free R_3Ga compounds can be obtained by mild thermal dissociation.

In this paper, full details are given of the synthesis and characterisation of these adducts, and structural data are presented for the adducts between Et_3Ga and Pr^i_3Ga and the macrocyclic N_4- and N_6-aza crown ligands. These compounds contain some of the longest [Ga–N] bonds reported to date, and are the first structurally characterised adducts of Et_3Ga and Pr^i_3Ga.

All compounds described herein are new, although a number of analogous adducts have been previously reported, including $(R_3M)_2$[MBDA] (M = In, R = Me, Et; M = Ga, R = Me; M = Al, R = Me),[6] $(Me_3Al)_4$[N_4-aza crown],[14] $(Me_3Ga)_4$[N_4-aza crown][14] and $(Me_3Ga)_4$[HMT] (where HMT = hexamethylenetetramine).[15]

2 Experimental

2.1 General techniques

The metalorganic compounds Et_3Ga and Pr^i_3Ga used in this study were supplied by Epichem Limited or were synthesised using standard Schlenk/vacuum line techniques. The nitrogen donor ligands used (Fig. 1) were triethylamine (Aldrich Chemical Co.), 4,4′-methylenebis(*N*,*N*′-dimethylaniline) [MBDA], 1,4,8,11-tetramethyl-1,4,8,11-tetraazacyclotetradecane (N_4-aza crown) and 1,4,7,10,13,16-hexamethyl-1,4,7,10,13,16-hexaazacyclooctadecane [N_6-aza crown]. All were purchased from Aldrich Chemical Co. and were dried by distillation over sodium wire and deoxygenated before use.

^{1}H NMR spectra were obtained using a Bruker 300 NMR spectrometer and infrared spectroscopy was carried out on a Perkin-Elmer 1000 infrared Fourier transform spectrometer using Nujol mulls between NaCl plates. Elemental microanalyses were carried out by the Chemistry Department service at Liverpool University.

2.2 Synthesis of $Pr^i_3Ga(NEt_3)$ and $Et_3Ga(NEt_3)$

A solution of gallium trichloride, $GaCl_3$ (1 mol equivalent), in pentane was added dropwise to a stirred solution of ethyl magnesium bromide (3.2 mol equiv.) or isopropylmagnesium bromide (3.2 mol equiv.) in triethylamine, NEt_3. After removal of excess NEt_3 *in vacuo*, the crude product was isolated by vacuum distillation (100 °C) into a receiver cooled in liquid nitrogen (*ca.* −196 °C). The $R_3Ga(NEt_3)$ adducts were purified by a further vacuum distillation (80 °C) into a cooled receiver (−196 °C).

Analysis of the adducts by ^{1}H NMR spectroscopy showed that Et_3Ga (NEt_3) had the predicted 1 : 1 stoichiometry, whilst the data for the $Pr^i_3Ga(NEt_3)$ adduct indicated a slight loss of NEt_3, with the adduct having the stoichiometry $Pr^i_3Ga(NEt_3)_{0.6}$.[8]

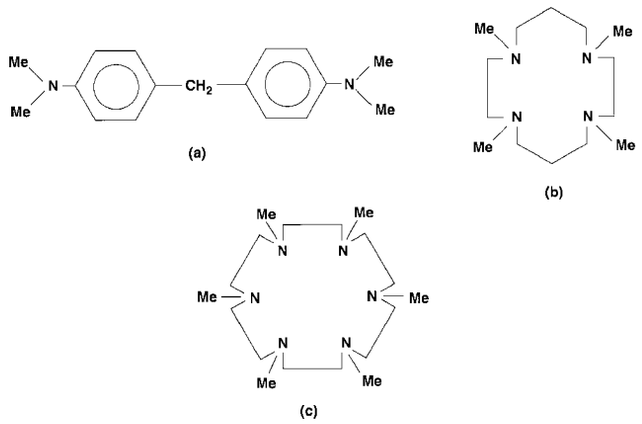

Fig. 1 Low volatility nitrogen donors used to displace NEt_3 from $Et_3Ga(NEt_3)$ and $Pr^i_3Ga(NEt_3)$: (a) MBDA, (b) N_4-aza crown, (c) N_6-aza crown.

$Et_3Ga(NEt_3)$. ^{1}H NMR (C_6D_6, 300 MHz, 20 °C): δ 0.4 [q, 6H, $GaCH_2CH_3$], 0.7 [t, 9H, $GaCH_2CH_3$], 1.4 [t, 9H, NCH_2CH_3], 2.2 [q, 6H, NCH_2CH_3].

$Pr^i_3Ga(NEt_3)_{0.6}$. ^{1}H NMR (C_6D_6, 300 MHz, 300 °C): δ 0.8 [t, 5.4H, NCH_2CH_3], 1.0 [m, 3H, $GaCH(CH_3)_2$], 1.4 [d, 18H, $GaCH(CH_3)_2$], 2.4 [q, 3.6H, NCH_2CH_3].

Further analysis of $Et_3Ga(NEt_3)$ and $Pr^i_3Ga(NEt_3)_{0.6}$ by inductively coupled plasma mass spectroscopy showed that *total* metal impurities in each compound were <1 ppm.

2.3 Synthesis of Et_3Ga and Pr^i_3Ga adducts with MBDA and cyclic aza-crown ligands

The same general synthesis method was used for compounds **1**–**7**. This involved the addition of the liquid adducts $Et_3Ga(NEt_3)$ (1 mol equiv.) or $Pr^i_3Ga(NEt_3)_{0.6}$ (1 mol equiv.) to a stirred suspension of the involatile nitrogen donor ligands in pentane; MBDA (0.5 mol equiv.), N_4-aza crown (0.25 mol equiv.) or N_6-aza crown (0.17 mol equiv.). Removal of the pentane and displaced NEt_3 *in vacuo* gave the adducts **1**–**7** as crystalline solids, or viscous liquids. The adducts were characterised by elemental microanalysis, infrared (IR) and ^{1}H NMR spectroscopy:

$(Et_3Ga)_2$[MBDA] (1). Colourless viscous liquid. ^{1}H NMR (C_6D_6, 300 MHz, 20 °C): δ 0.45 [q, 12H, $GaCH_2CH_3$], 1.28 [t, 18H, $GaCH_2CH_3$], 2.25 [s, 12H, NCH_3], 3.63 [s, 2H, CH_2], 6.82 [m, 8H, C_6H_4]. Anal. found: C, 60.27; H, 9.42; N, 5.17; calc. for $C_{29}H_{52}N_2Ga_2$: C, 61.29; H, 9.22; N, 4.93%.

$(Pr^i_3Ga)_2$[MBDA] (2). Pale yellow viscous liquid. ^{1}H NMR (C_6D_6, 300 MHz, 20 °C): δ 0.95 [t, 6H, $GaCH(CH_3)_3$], 1.3 [d, 36H, $GaCH(CH_3)_2$], 2.43 [s, 12H, NCH_3], 3.70 [s, 2H, CH_2], 6.88 [m, 8H, C_6H_4]. Anal. found: C, 65.10; H, 10.24; N, 5.33; calc. for $C_{35}H_{64}N_2Ga_2$: C, 64.42; H, 9.89; N, 5.33%.

$(Et_3Ga)_4$[N_4-aza crown] (3). Colourless crystalline solid, mp 123–125 °C. ^{1}H NMR (C_6D_6, 300 MHz, 20 °C): δ 0.56 [q, 24H, $GaCH_2CH_3$], 1.5 [t, 36H, $GaCH_2CH_3$], 1.84 [s, 12H, NCH_3], 2.26 [bs, 20H, $NCH_2CH_2CH_2N$, NCH_2CH_2N]. Anal. found: C, 51.00; H, 10.39; N, 5.73; calc. for $C_{38}H_{92}N_4Ga_4$: C, 51.62; H, 10.49; N, 6.34%. IR (Nujol) ν/cm^{-1}: 3642w, 997m, 804w, 652m, 526s.

$(Pr^i_3Ga)_4$[N_4-aza crown] (4). Colourless crystalline solid, mp 83–84 °C. ^{1}H NMR (C_6D_6, 300 MHz, 20 °C): δ 1.04 [m, 12H, $GaCH(CH_3)_2$], 1.5 [d, 72H, $GaCH(CH_3)_2$], 1.98 [s, 12H, NCH_3], 2.35 [m, 20H, $NCH_2CH_2CH_2N$, NCH_2CH_2N]. Anal. found; C, 57.73; H, 11.41; N, 7.61; calc. for $C_{50}H_{116}N_4Ga_4$: C, 57.06; H, 11.11; N, 5.33%. IR (Nujol) ν/cm^{-1}: 3500vw, 1296w, 1266w, 1222w, 1178m, 1127w, 1101w, 1059m, 1026m, 962s, 868m, 833w, 796vw, 724w.

$(Et_3Ga)_4$[N_6-aza crown] (5). Crystals of this stoichiometry were obtained by slow recrystallisation of the $(Et_3Ga)_6$[N_6-aza crown] adduct, and were only characterised by X-ray diffraction.

$(Et_3Ga)_6$[N_6-aza crown] (6). Colourless crystalline solid, mp 103–104 °C. ^{1}H NMR (C_6D_6, 300 MHz, 20 °C): δ 0.6 [q, 36H, $GaCH_2CH_3$], 1.49 [t, 54H, $GaCH_2CH_3$] 2.07 [s, 18H, NCH_3], 2.46 [bs, 24H, NCH_2CH_2N]. Anal. found: C, 50.88; H, 10.60; N, 7.29; calc. for $C_{54}H_{132}N_6Ga_6$: C, 50.51; H, 10.36; N, 6.55%. IR (Nujol) ν/cm^{-1}: 3643w, 1307m, 1233w, 1127m, 1029s, 999s, 958s, 770w, 723w, 652m, 564s, 514s.

($Pr^i_3Ga)_4[N_6$-aza crown] (7). Colourless crystalline solid, mp 75–76 °C. ^{1}H NMR (C_6D_6, 300 MHz, 20 °C): δ 1.04 [m, 12H, GaC*H*$(CH_3)_2$], 1.5 [d, 72H, GaCH$(CH_3)_2$], 1.98 [s, 18H, NCH_3], 2.52 [t, 24H, NCH_2CH_2N]. Anal. found: C, 56.81; H, 11.49; N, 8.00; calc. for $C_{54}H_{126}N_6Ga_4$: C, 56.95; H, 11.18; N, 7.38%. IR (Nujol) ν/cm^{-1}: 1315m, 1216w, 1121m, 1070m, 1020s, 996s, 923s, 869m, 812m, 766w.

2.4 Single crystal X-ray diffraction

Single crystals of $(Et_3Ga)_4[N_4$-aza crown] (**3**), $(Pr^i_3Ga)_4[N_4$-aza crown] (**4**), $(Et_3Ga)_4[N_6$-aza crown] (**5**), $(Et_3Ga)_6[N_6$-aza crown] (**6**) and $(Pr^i_3Ga)_4[N_6$-aza crown] (**7**) suitable for X-ray diffraction were obtained by the slow recrystallisation of each adduct from hexane.

Crystallographic data for **4** to **6** were recorded on a Stoe IPDS diffractometer using graphite monochromated Mo-Kα radiation ($\lambda = 0.71073$ Å), $T = 200$ K. Crystallographic data for **3** and **7** were recorded on a Bruker-AXS P4 diffractometer using graphite monochromated Mo-Kα radiation ($\lambda = 0.71073$ Å), $T = 223$ K. Structures were solved by direct methods and refined by full-matrix least squares against F^2 using all data.[16] Non-hydrogen atoms have been refined anisotropically, with the exception of disordered groups, which were refined isotropically (one Et_3Ga, one ethyl and two methyl groups in **6** were disordered and split on two positions in the refinement using distance and ADP restraints). Hydrogen positions were set geometrically. Crystal and data collection parameters for compounds **3**–**7** are given in Table 1.

CCDC reference number 1145/224. See http://www.rsc.org/suppdata/jm/b0/b001937m/ for crystallographic files in .cif format.

3 Results and discussion

Elemental microanalysis data for the adducts shows that the MBDA and N_4-aza crown adducts have the predicted 2 : 1 and 4 : 1 R_3Ga : ligand stoichiometry, and the molecular structures of **3** and **4** are shown in Fig. 2 and 3. In contrast, the R_3Ga adducts with the N_6-aza crown ligand display varying stoichiometries of either 4 : 1 or 6 : 1, due to steric constraints on the N_6 core. For instance, Et_3Ga forms two types of adducts, $(Et_3Ga)_4[N_6$-aza crown] (Fig. 4) and $(Et_3Ga)_6[N_6$-aza crown] (Fig. 5). It is significant that the 6 : 1 stoichiometry is observed only when Et_3Ga is present in excess during the recrystallisation process. Reference to Fig. 5 shows that there is a considerable degree of steric crowding in the $(Et_3Ga)_6[N_6$-aza crown] molecule, so that under less forcing conditions, only four Et_3Ga molecules coordinate to the N_6-aza crown ligand. It is significant that in order to accommodate six Et_3Ga molecules around the N_6 core, the R_3Ga moieties coordinate alternately above and below the plane of the aza crown, whilst the flexible ethyl groups distort to minimise steric crowding. However, the large steric bulk and extra rigidity of the isopropyl group precludes coordination of all six Pr^i_3Ga molecules to the N_6-aza crown nitrogen core and the only complex present, even when Pr^i_3Ga is in excess, is the 4 : 1 adduct $(Pr^i_3Ga)_4[N_6$-aza crown] (see Fig. 6).

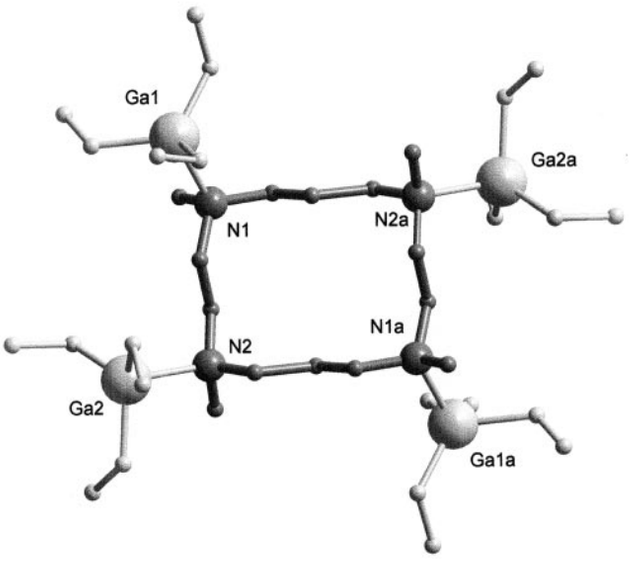

Fig. 2 Crystal structure of $(Et_3Ga)_4[N_4$-aza crown] (**3**).

There are very few reports of adducts between Et_3Ga, Pr^i_3Ga and tertiary amines and there is a complete absence of structural data. However, a number of Me_3Ga–amine adducts have been structurally characterised, including (Me_3Ga)[HMT],[17] $(Me_3Ga)_2$[HMT],[17] $(Me_3Ga)_4$[HMT],[15] $(Me_3Ga)_4[N_4$-aza crown],[14] $(Me_3Ga)_2[N(C_2H_4)N]$,[18] $Me_3Ga[NH(C_6H_{11})_2]$[19] and Me_3Ga[NHCHMe$(CH_2)_3$CHMe].[19] Selected bond distances and bond angles for compounds **3** and **4** are given in Table 2, and those for the adducts **5**–**7** are summarised in Table 3.

All of the adducts contain 4-coordinate Ga atoms, with the R_3Ga molecules exhibiting distorted tetrahedral geometry, similar to the geometry in the analogous adduct $(Me_3Ga)_4[N_4$-aza crown],[14] and in other R_3Ga–tertiary amine adducts, such as $(Me_3Ga)_2[N(C_2H_4)_3N]$[19] and $(Me_3Ga)_4$[HMT].[15] The C–Ga–N bond angles in **3** and **4** are generally less than the tetrahedral angle of 109° and range from 100–107.5°. These values are comparable to the C–Ga–N values in $(Me_3Ga)_4[N_4$-aza crown] (101.0–105.9°), $(Me_3Ga)_2[N(C_2H_4)N]$ (101.4,

Table 1 Crystal and data collection parameters for $(Et_3Ga)_4[N_4$-aza crown] (**3**), $(Pr^i_3Ga)_4[N_4$-aza crown] (**4**), $(Et_3Ga)_4[N_6$-aza crown] (**5**), $(Et_3Ga)_6[N_6$-aza crown] (**6**) and $(Pr^i_3Ga)_4[N_6$-aza crown] (**7**)

	3	**4**	**5**	**6**	**7**
Empirical formula	$C_{38}H_{92}Ga_4N_4$	$C_{50}H_{116}Ga_4N_4$	$C_{42}H_{102}Ga_4N_6$	$C_{54}H_{132}Ga_6N_6$	$C_{54}H_{126}Ga_4N_6$
Formula weight	884.04	1052.58	970.38	1284.24	1138.49
a/Å	8.8976(9)	8.7237(13)	9.2460(15)	11.706(4)	10.5918(17)
b/Å	11.6366(11)	12.880(2)	10.902(2)	13.370(3)	22.387(3)
c/Å	11.7629(8)	13.649(2)	13.421(3)	23.081(4)	14.0306(19)
α/°	83.338(7)	101.558(18)	74.15(2)	104.64(2)	90
β/°	88.446(7)	92.290(18)	81.74(2)	90.77(4)	104.297(13)
γ/°	82.189(8)	105.696(18)	85.47(2)	103.13(4)	90
V/Å^3	1198.38(18)	1439.3(4)	1286.8(4)	3394.2(16)	3223.9(8)
Crystal system	triclinic	triclinic	triclinic	triclinic	monoclinic
Space group	$P\bar{1}$	$P\bar{1}$	$P\bar{1}$	$P\bar{1}$	$P2_1/n$
Z	1	1	1	2	2
Refl. collected	6506	9194	6480	18258	8915
Refl. unique (R_{int})	5460 (0.0211)	4271 (0.0505)	3801 (0.0948)	8421 (0.0464)	7326 (0.0403)
*R*1 [$I > 2\sigma(I)$]	0.0337	0.0395	0.0409	0.0366	0.0436
*wR*2 (all data)	0.0763	0.0983	0.1020	0.0906	0.1104

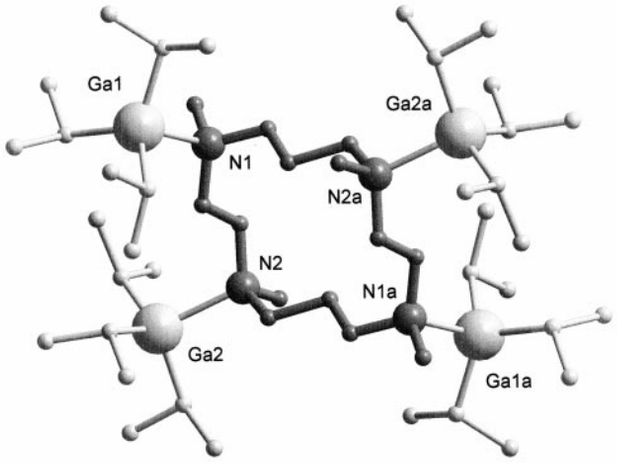

Fig. 3 Crystal structure of $(Pr^i_3Ga)_4[N_4$-aza crown] (**4**).

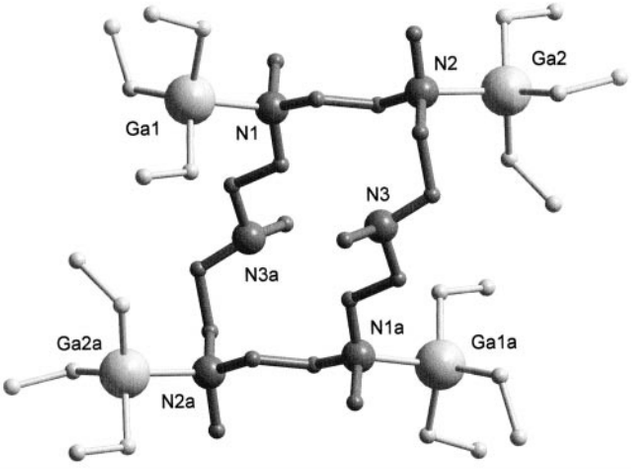

Fig. 4 Crystal structure of $(Et_3Ga)_4[N_6$-aza crown] (**5**).

100.5°) and $(Me_3Ga)_4$[HMT] (96.7–111.1°). In **3** and **4** the C–Ga–C bond angles range from 111.4 to 118.0°, similar to the C–Ga–C angles in $(Me_3Ga)_4[N_4$-aza crown] (113.0–118.1°) and $(Me_3Ga)_2[N(C_2H_4)N]$ (116.2, 116.8°), but show less spread in values than the C–Ga–C angles in $(Me_3Ga)_4$[HMT] (110.1–120.6°).[15] In the N_4- and N_6-aza crown adducts, the Ga–C bond lengths tend to increase in the order Ga–Me (typically

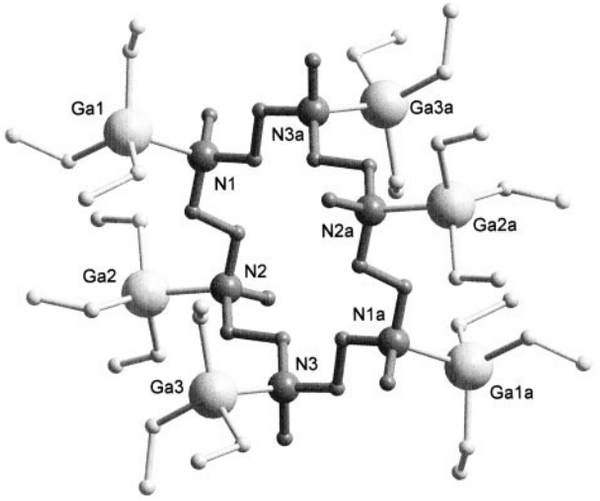

Fig. 5 Crystal structure of $(Et_3Ga)_6[N_6$-aza crown] (**6**).

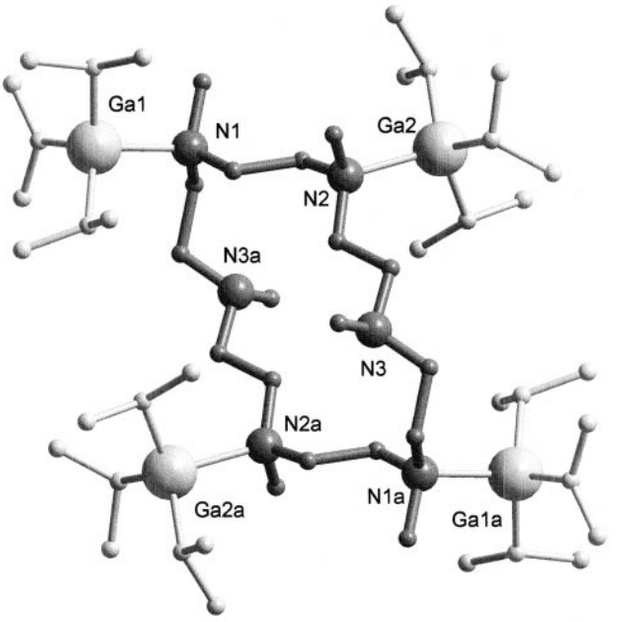

Fig. 6 Crystal structure of $(Pr^i_3Ga)_4[N_6$-aza crown] (**7**).

1.96 Å) < Ga–Et (2.0 Å) < Ga–Pr^i (2.02 Å) (see data in Tables 3 and 4), consistent with a decrease in Ga–C bond strength in the order $Me_3Ga > Et_3Ga > Pr^i_3Ga$.

The Et_3Ga and Pr^i_3Ga molecules also display distorted tetrahedral configuration in the N_6-aza crown adducts, with similar C–Ga–N angles (Et_3Ga: 99.9–106.66°; Pr^i_3Ga: 102.94–105.80°) and C–Ga–C angles (Et_3Ga: 112.2–119.0°; Pr^i_3Ga: 110.96–116.8°) to those in the N_4-aza crown adducts (see Table 3). However, the Ga–N bond lengths were found to depend strongly on the nature of R_3Ga and the stoichiometry of the adduct. In Table 4, the Ga–N bond distance in **3**–**7** are compared with the Ga–N distance in the analogous adduct $(Me_3Ga)_4[N_4$-aza crown] and a number of other R_3Ga–tertiary amine adducts. The data show that the Ga–N bond distances are smallest in the least sterically hindered adducts, such as (Me$_3$Ga)[HMT] (2.14 Å) and $(Me_3Ga)_2[N(C_2H_4)N]$ (2.15, 2.16 Å). Increased steric hindrance around the nitrogen core of the macrocyclic amine leads to a marked lengthening of the

Table 2 Selected bond distances (Å) and angles (°) for $(Et_3Ga)_4[N_4$-aza crown] (**3**) and $(Pr^i_3Ga)_4[N_4$-aza crown] (**4**)

$(Et_3Ga)_4[N_4$-aza crown]	$(Pr^i_3Ga)_4[N_4$-aza crown]
Ga(1)–C(11) 1.995(3)	Ga(1)–C(17) 2.007(5)
Ga(1)–C(12) 1.995(3)	Ga(1)–C(11) 2.018(5)
Ga(1)–C(13) 1.997(3)	Ga(1)–C(14) 2.031(4)
Ga(2)–C(21) 1.996(2)	Ga(2)–C(24) 2.005(5)
Ga(2)–C(23) 1.996(2)	Ga(2)–C(27) 2.005(4)
Ga(2)–C(22) 2.000(3)	Ga(2)–C(21) 2.010(5)
Ga(1)–N(1) 2.205(2)	Ga(1)–N(1) 2.293(3)
Ga(2)–N(2) 2.2197(19)	Ga(2)–N(2) 2.264(3)
C(11)–Ga(1)–C(12) 116.50(15)	C(17)–Ga(1)–C(11) 118.0(2)
C(11)–Ga(1)–C(13) 116.87(16)	C(17)–Ga(1)–C(14) 114.21(19)
C(12)–Ga(1)–C(13) 112.95(13)	C(11)–Ga(1)–C(14) 113.20(18)
C(21)–Ga(2)–C(23) 114.59(11)	C(24)–Ga(2)–C(27) 111.4(2)
C(21)–Ga(2)–C(22) 116.90(12)	C(24)–Ga(2)–C(21) 111.79(19)
C(23)–Ga(2)–C(22) 113.93(11)	C(27)–Ga(2)–C(21) 117.25(18)
C(11)–Ga(1)–N(1) 101.09(11)	C(17)–Ga(1)–N(1) 100.01(15)
C(12)–Ga(1)–N(1) 102.83(11)	C(11)–Ga(1)–N(1) 101.50(16)
C(13)–Ga(1)–N(1) 103.65(12)	C(14)–Ga(1)–N(1) 107.50(15)
C(21)–Ga(2)–N(2) 101.55(9)	C(24)–Ga(2)–N(2) 106.46(15)
C(23)–Ga(2)–N(2) 101.48(9)	C(27)–Ga(2)–N(2) 106.72(16)
C(22)–Ga(2)–N(2) 105.73(10)	C(21)–Ga(2)–N(2) 102.05(15)

Table 3 Selected bond distances (Å) and bond angles (°) in $(Et_3Ga)_4[N_6$-aza crown] (**5**),$(Et_3Ga)_6[N_6$-aza crown] (**6**) and $(Pr^i{}_3Ga)_4[N_6$-aza crown] (**7**)

$(Et_3Ga)_4[N_6$-aza crown] (**5**)	$(Et_3Ga)_6[N_6$-aza crown] (**6**)	$(Pr^i{}_3Ga)_4[N_6$-aza crown] (**7**)
Ga(1)–C(14) 1.984(5)	Ga(1)–C(14) 1.987(5)	Ga(1)–C(12) 2.017(3)
Ga(1)–C(18) 2.011(4)	Ga(2)–C(26) 1.991(5)	Ga(1)–C(13) 2.021(3)
	Ga(3)–C(38) 1.997(5)	Ga(1)–C(11) 2.023(3)
	Ga(4)–C(44) 1.992(5)	Ga(2)–C(21) 1.997(4)
	Ga(5)–C(58) 2.026(11)	Ga(2)–C(22) 2.018(3)
	Ga(6)–C(66) 1.996(5)	Ga(2)–C(23) 2.022(3)
Ga(1)–N(1) 2.212(4)	Ga(1)–N(1) 2.258(3)	Ga(1)–N(1) 2.263(2)
Ga(2)–N(2) 2.206(4)	Ga(5)–N(5) 2.074(8)	Ga(2)–N(2) 2.247(2)
C(14)–Ga(1)–C(18) 119.0(2)	C(18)–Ga(1)–C(16) 113.8(2)	C(21)–Ga(2)–C(23) 110.96(17)
C(16)–Ga(1)–C(18) 112.2(2)	C(26)–Ga(2)–C(24) 116.7(2)	C(21)–Ga(2)–C(22) 116.8(2)
	C(34)–Ga(3)–C(36) 113.9(2)	
	C(46)–Ga(4)–C(44) 116.2(2)	
	C(56)–Ga(5)–C(58) 113.3(5)	
	C(64)–Ga(6)–C(66) 114.1(3)	
C(14)–Ga(1)–N(1) 99.90(17)	C(16)–Ga(1)–N(1) 105.38(18)	C(11)–Ga(1)–N(1) 105.80(10)
C(26)–Ga(2)–N(2) 106.66(18)	C(24)–Ga(2)–N(2) 105.56(17)	C(23)–Ga(2)–N(2) 102.94(11)
	C(34)–Ga(3)–N(3) 101.4(2)	
	C(44)–Ga(4)–N(4) 100.97(18)	
	C(64)–Ga(6)–N(6) 106.1(2)	

Ga–N bond. For instance, the Ga–N bond distance increases from 2.20, 2.21 Å in $(Et_3Ga)_4[N_6$-aza crown] to 2.22, 2.26 Å in $(Et_3Ga)_6[N_6$-aza crown] as more Et_3Ga molecules are packed around the N_6 core. A similar effect occurs on going from $(Me_3Ga)_2$[HMT] (Ga–N = 2.138 Å) to $(Me_3Ga)_4$[HMT] (Ga–N = 2.26, 2.32 Å).

For a given aza crown ligand, the Ga–N bond distance in the adduct increases in the order $Me_3Ga < Et_3Ga < Pr^i{}_3Ga$, *e.g.* $(Me_3Ga)_4[N_4$-aza crown] (Ga–N = 2.18, 2.20 Å) < $(Et_3Ga)_4[N_4$-aza crown] (Ga–N = 2.20, 2.22 Å) < $(Pr^i{}_3Ga)_4[N_4$-aza crown] (Ga–N = 2.26, 2.29 Å) and $(Et_3Ga)_4[N_6$-aza crown] (Ga–N = 2.21 Å) < $(Pr^i{}_3Ga)_4[N_6$-aza crown] (2.25, 2.26 Å).

The Ga–N bond distances in compounds **3**–**7** range over 2.206–2.293 Å which are some of the longest yet reported. The Ga–N bond distance of 2.293(3) Å in **4** is very close to the longest reported Ga–N distance [2.318(9) Å] in $(Me_3Ga)_4$[HMT]. This strongly suggests that these R_3GaN_4- and N_6-aza crown adducts have relatively weak Ga–N bonds. This has important implications for their utility in the adduct purification process since, for effective use in the isolation of base-free R_3Ga and R_3In compounds, it is essential that the group III–trialkyl amine adducts dissociate at moderate temperatures (*i.e.* < 160 °C). It is important that the adduct dissociates at a significantly lower temperature than the distillation temperature of the amine ligand, otherwise isolation of the pure group III trialkyl species will be difficult.

Table 4 Comparison of Ga–N bond distances (Å) in a variety of R_3Ga–amine adducts

Compound	Ga–N	Reference
$(Et_3Ga)_4[N_4$-aza crown] (**3**)	2.205(2)	This work
	2.2197(19)	
$(Pr^i{}_3Ga)_4[N_4$-aza crown] (**4**)	2.293(3)	This work
	2.264(3)	
$(Et_3Ga)_4[N_6$-aza crown] (**5**)	2.212(4)	This work
	2.206(4)	
$(Et_3Ga)_6[N_6$-aza crown] (**6**)	2.258(3)	This work
	2.224(3)	
$(Pr^i{}_3Ga)_4[N_6$-aza crown] (**7**)	2.263(2)	This work
	2.247(2)	
$(Me_3Ga)_4[N_4$-aza crown]	2.182(4)	13
	2.202(4)	
(Me_3Ga)[HMT]	2.14(17)	15
$(Me_3Ga)_2$[HMT]	2.138(9)	15
$(Me_3Ga)_4$[HMT]	2.263(10)–2.2318(9)	14
$(Me_3Ga)_2[N(C_2H_4)N]$	2.154(9)	16
	2.164(9)	
$(Me_3Ga)[NH(C_6H_{11})_2]$	2.151(6)	17

Thermal dissociation was carried out by heating the adducts *in vacuo*, with the liberated R_3Ga compound being collected in a cooled receiver (*ca.* −196 °C). The identity of the liberated R_3Ga compound was, in each case, confirmed by proton NMR analysis and it was found that all adducts gave quantitative yields (> 80%) of base-free R_3Ga at low/moderate temperatures (*ca.* 75–140 °C). Significantly, the $(Me_3Ga)_2[N(C_2H_4)N]$ adduct was reported[18,19] to sublime unchanged, without dissociation at temperatures of 60 °C *in vacuo*, despite the presence of relatively long Ga–N bonds (2.154, 2.164 Å).[18] This is consistent with the proposal[6] that the presence of a methyl group attached to the donor nitrogen facilitates adduct dissociation by increasing steric hindrance in the molecule, and this is supported by separate dissociation studies[20] on $(Et_3Ga)_2$[2,2′-bipyridyl] and $(Et_3Ga)_2$[4,4′-bipyridyl] which showed them to be thermally stable up to 190 °C.

Although a major application of these Group III alkyl–MBDA and aza crown adducts is the isolation of base-free R_3M compounds from tertiary amine solvents, their use is by no means restricted to this application. Low volatility tertiary amines, such as MBDA, have already been used[6] as alternatives to conventional adducts, such as DIPHOS, in conventional ether-based reaction media, and a further advantage we have identified is that they allow the complete removal of alkyl halide impurities by precipitating them as involatile quaternary ammonium salts, $R_4N^+X^-$. This is a potentially useful function, as alkyl halides are common impurities in R_3M compounds prepared from $RMgX–MX_3$ Grignard reactions.[4] A particular feature to note is that the route involves *two* adduct purification steps, with trace metal impurities being readily removed from the $R_3Ga(NEt_3)$ adduct formed *in situ*, followed by a second purification stage in which trace metal impurities can be removed from the $(R_3Ga)_xL$ adduct.

Growth of AlGaAs by CBE using $Pr^i{}_3Ga$

The use of $Pr^i{}_3Ga$ in place of Et_3Ga has previously been shown to lead to a significant reduction in carbon contamination in AlGaAs grown by CBE. However, the presence of trace oxygen is particularly damaging to device performance in Al-containing III–V materials. It is therefore important to remove potential oxygen contaminants from the group III precursor.

Preliminary investigations[13] into the growth of $Al_{0.3}Ga_{0.7}As$ by CBE using base-free Pr^i_3Ga (prepared in NEt_3 and isolated using MBDA) and $AlH_3(NMe_2Et)$ showed that oxygen levels were at or below the SIMS detection limit of 1×10^{17} cm^{-3}, comparable to the best results obtained on the same reactor using Et_3Ga or the $Pr^i_3Ga(NEt_3)_{0.6}$ adduct.[8] The low oxygen content of the AlGaAs layers resulting from the Pr^i_3Ga/$AlH_3(NMe_2Et)$ precursor combination gave rise to films with good photoluminescence properties. A 10 nm GaAs/$Al_{0.3}Ga_{0.7}As$ quantum well grown at the relatively low growth temperature of 540 °C gave a carrier lifetime of 1 ns, comparable to the best results obtained on the same reactor using Et_3Ga. These were entirely reproducible results and were obtained using three separate batches of base-free Pr^i_3Ga synthesised in trialkylamine media, fully demonstrating the practical utility of amine-based synthesis routes.

4 Conclusions

The metalorganic precursors Et_3Ga and Pr^i_3Ga have been synthesised without the use of oxygen-containing ether solvents. The base-free compounds were obtained from the $R_3Ga(NEt_3)$ adducts by the addition of low volatility bidentate or multidentate nitrogen donors, followed by thermal dissociation of the resulting amine adducts. SIMS and carrier lifetime measurements on AlGaAs grown by CBE using base-free Pr^i_3Ga synthesised by these new techniques show that the layers are "state of the art", with some of the lowest carbon and oxygen levels reported in CBE-grown material. Further work is underway, aimed at extending these ether-free synthesis and purification techniques to MOVPE precursors such as Me_3In and Me_3Ga.

Acknowledgements

The authors are grateful to Epichem Limited for funding the work. We thank J. O. Maclean, R. S. Balmer and T. Martin for provision of the AlGaAs growth data, S. A. Apter (University of Liverpool, UK) for the microanalyses, and J. R. Thompson for assistance with crystal structures (**3**) and (**7**).

References

1 G. B. Stringfellow, *Organometallic Vapor Phase Epitaxy: Theory and Practice*, Academic Press, New York, 1989.
2 A. C. Jones and P. O'Brien, *CVD of Compound Semiconductors*, VCH, Weinheim, 1997.
3 A. C. Jones, *Chem. Br.*, 1995, **31**, 389.
4 A. C. Jones, A. K. Holliday, D. J. Cole-Hamilton, M. M. Ahmad and N. D. Gerrard, *J. Crystal Growth*, 1984, **68**, 1.
5 D. C. Bradley, H. Chudzynska, M. M. Faktor, D. M. Frigo, M. B. Hursthouse, B. Hussain and L. M. Smith, *Polyhedron*, 1988, **7**, 1289.
6 D. F. Foster, S. A. Rushworth, D. J. Cole-Hamilton, A. C. Jones and J. P. Stagg, *Chemtronics*, 1988, **3**, 38.
7 H. Terao and H. Sunakawa, *J. Crystal Growth*, 1984, **68**, 157.
8 R. W. Freer, T. J. Whitaker, T. Martin, P. D. J. Calcott, M. Houlton, D. Lee, A. C. Jones and S. A. Rushworth, *Adv. Mater.*, 1995, **7**, 478.
9 J. S. Roberts, J. P. R. David, L. Smith and P. L. Tihanyi, *J. Crystal Growth*, 1998, **195**, 668.
10 K. Yasuda and R. Okawara, *Organomet. Chem. Rev.*, 1967, **2**, 255.
11 E. C. Ashby and F. W. Walker, *J. Org. Chem.*, 1968, **10**, 3821.
12 T. J. Whitaker, R. W. Freer, T. Martin, A. C. Jones and S. A. Rushworth, *J. Electron. Mater.*, 1996, **25**, 1060.
13 K. M. Coward, A. C. Jones, M. E. Pemble, S. A. Rushworth, L. M. Smith and T. Martin, *J. Electron. Mater.*, 2000, **29**, 152.
14 B. Lee, W. T. Pennington, G. H. Robinson and R. D. Rogers, *J. Organomet. Chem.*, 1990, **396**, 269.
15 J. B. Hill, S. J. Eng, W. T. Pennington and G. H. Robinson, *J. Organomet. Chem.*, 1993, **445**, 11.
16 G. M. Sheldrick, SHELX-97, Programs for Crystal Structure Solution and Refinement, University of Gottingen, Germany, 1997.
17 H. Krause, K. Sille, H.-D. Hausen and J. Weidlein, *J. Organomet. Chem.*, 1982, **235**, 253.
18 A. M. Bradford, D. C. Bradley, M. B. Hursthouse and M. Motevalli, *Organometallics*, 1992, **11**, 111.
19 D. C. Bradley, H. M. Dawes, M. B. Hursthouse, L. M. Smith and M. Thornton-Pett, *Polyhedron*, 1990, **9**, 343.
20 K. M. Coward and A. C. Jones, unpublished results, 1998.